Tough, Thin Hydrogel Membranes with Giant Crystalline Domains Composed of Precisely Synthesized Macromolecules

Tatsuo Kaneko,[†,‡] Shinji Tanaka,[‡,§] Atsuhiko Ogura,[§] and Mitsuru Akashi*[,†,‡]

Department of Applied Chemistry, Graduate School of Engineering, Osaka University, 2-1, Yamadaoka, Suita 565-0871, Japan; Department of Nanostructured and Advanced Materials, Graduate School of Science and Engineering, Kagoshima University, 1-21-40, Korimoto, Kagoshima 890-0065, Japan; and Tsukuba Research Laboratory, NOF Corporation, 5-10 Tokodai, Tsukuba 300-2635, Japan

Received January 20, 2005; Revised Manuscript Received March 8, 2005

ABSTRACT: ABA-type triblock copolymers, poly{(γ-benzyl L-aspartate) (BLA)-*block*-ethylene oxide (EO)-*block*-BLA}, with a controlled chain length were prepared. The copolymer film (ca. 0.01 mm thickness) was immersed into the water to create a thin, self-sustainable hydrogel membrane (0.01−0.02 mm thickness) that was largely deformable and tough in its equilibrated water-swollen state (water content: 58−83 wt %). Crossed-polarizing microscopy confirmed that the water-swollen membrane had a framework of giant crystalline domains 10 μm−4 mm in size; as far as we know, crystalline domains large enough to observe by an optical microscope in the hydrogels have never been reported. During the water-swelling process, the triblock copolymers showed an α-helix−β-strand transformation of their PBLA blocks and long-range structural formation, which may have reinforced the hydrogel thin membrane, thus increasing its toughness.

Introduction

Hydrogels are soft materials composed of a fluid-filled network that can transport solvent-soluble molecules, just like in living organisms.[1] Most biological gels form well-ordered aggregates[2] which sometimes arrange themselves regularly in a continuous length beyond the micrometer scale and allow living materials such as muscular tissue to be of sufficient mechanical toughness. On the other hand, synthetic hydrogels have serious problems restraining their application, such as mechanical weakness. There are several studies on the preparation of strong, chemically cross-linked hydrogels generated by constructing a double-network architecture[3] and a crystalline nanodomain.[4] The contact lens for correcting eyesight is a representative hydrogel membrane (thickness > 0.1 mm) tough enough to use actually. However, as far as we know, there have been no reports on the preparation of thin (thickness < 0.05 mm), strong hydrogel membranes generated by a chemical cross-linking method, which requires the difficult process of completely removing the unreacted monomers, cross-linkers, initiators, and other reagents, which may sometimes have deleterious effects on membrane function. On the other hand, the self-assembly of macromolecular chains can yield physically cross-linked hydrogels with no impurities, such as regenerated cellulose membranes, that are strong enough to be used for dialysis in water.[5] The nanoscaled crystalline domains lie scattered throughout the regenerated celluloses membrane.[5] On the basis of a biomimetic concept, we can hypothesize that physical hydrogels with crystalline domains arranged in long-range continuous lengths may form extremely tough, thin hydrogel membranes.

In a previous paper, we synthesized an ABA-type triblock copolymer comprised of poly(γ-benzyl L-aspartate) (PBLA) as a hydrophobic (A) segment and poly(ethylene oxide) (PEO, number-average molecular weight, M_n = 20 300) as a hydrophilic (B) segment.[6] The copolymers had monodispersed chain lengths and excellent cell compatibility.[7] Although ABA-type triblock copolymers containing PEO as a B block were widely studied and the importance of interblock interactions on the mutual crystallization behavior following thermal treatment has been reported,[8] there are no reports on block copolymers containing long PEO blocks with a polymerization degree (PD) of more than 200, except for ours. When we made previous studies of cell compatibility on the poly(BLA-*block*-EO-*block*-BLA) films with more than 0.1 mm thickness, the high toughness was confirmed. Although the thick films gave an ease to make the cell adhesion test, they were not suitable for the structural investigation by optical microscopy and X-ray diffraction. This result motivated us to reduce the thickness keeping the high toughness and to obtain the structural characteristics. Here we report the in situ hydrogelation of triblock PBLA−PEO−PBLA copolymer thin films (thickness: 0.01 mm) with long PEO blocks (PD = 460), which would be expected to swell a large amount of water and easily to confirm the crystalline structure. We successfully formed the very tough but thin hydrogels membranes by controlling the moisture and found that the copolymers showed a water-induced polypeptide transformation and formed giant spherullite domains with long-range ordering.

Experimental Section

Materials. PEO with amino groups at both ends is commercially available (M_n = 20 300, NOF Corp., Japan) and was used as received as the initiator of the polymerization of β-benzyl L-aspartate *N*-carboxyanhydride (BLA-NCA). Dehydrated dichloromethane (Kanto Kagaku, Japan) and *N*,*N*-dimethylformamide (DMF, water content <30 ppm, Wako Chemical Co. Ltd., Japan) were used for the polymerization

† Osaka University.
‡ Kagoshima University.
§ NOF Corporation.
* Corresponding author: Tel +81-6-6879-7356; Fax +81-6-6879-7359; e-mail akashi@chem.eng.osaka-u.ac.jp.

10.1021/ma050121p CCC: $30.25
Published on Web 04/30/2005

as received. BLA-NCA was prepared by the method of Goodman et al.,[9] and poly(BLA-*block*-EO-*block*-BLA) triblock copolymers were prepared in the previously reported procedure.[6,7]

Hydrogel Preparation. Hydrogels formed from poly(BLA-*block*-EO-*block*-BLA) triblock copolymers were prepared by an in situ gelation method as follows. The dry films were prepared by casting from a dichloromethane solution (3 mL, 1% w/v) of PBLA−PEO−PBLA triblock copolymers on a flat Teflon dish (diameter: 50 mm), and the dichloromethane was spontaneously vaporized at 25 °C under conditions free from moisture in desiccators. The central part of the dry films were cut into rectangular shapes (30 mm × 30 mm) and then swollen in a large amount of pure water at 25 °C for over 1 h, yielding flexible hydrogels. The dry sample was weighed (w_{dry}) prior to the hydrogel formation, and the swollen films were weighed (w_{gel}) after the excess water on the film surface was removed. The swelling ratio, q, was determined according to the following equation: $q = w_{gel}/w_{dry}$.

Measurements. Crossed-polarizing microscopic images were taken with an Olympus BX51 microscope equipped with a digital camera and a programmable temperature controller (resolution: ±0.1 K). The studies of differential scanning calorimetry (DSC) were made using a Seiko Instrument Inc. DSC-210. All experiments were performed in a nitrogen gas atmosphere in the temperature range from 20 to 95 °C at a heating rate of 10 °C min^{-1}. The hydrogel specimens were hermetically sealed with water in the aluminum pan. X-ray diffraction patterns (XRD) were recorded on an X-ray diffractometer (RINT UltraX18) equipped with a scintillation counter using Cu Kα radiation (40 kV, 200 mA; wavelength = 1.5418 Å), which was monochromated by a parabolic multilayer mirror in transmission geometry. The stress−strain curve of a strip of film 2 mm wide was measured by a Yamaden creep meter RE3305 at room temperature at a tensile rate of 1.0 cm min^{-1}. Young's modulus was determined from the inclination of the curve within a strain of less than 1%. The transmission electron microscopic (TEM) image of stained ultrathin cross sections for dry polymer film was measured by Hitachi H-7100FA TEM operated at an acceleration voltage of 100 kV. The freeze-dried film embedded in the epoxide resin was cut with a diamond knife (DiATOME ULTRA Cryo Dry) in a ultramicrotome system (Leica EM-Ultracut-UCT, EM-FCS cryosystem) to yield ultrathin cross sections with less than 0.1 μm thickness as a TEM specimen. The sections were put on a cupper mesh and dried under reduced pressure. The obtained specimens were stained by a vapor of ruthenium tetraoxide.

Results and Discussion

1. Hydrogel Preparation. We used the previously reported PBLA−PEO−PBLA triblock copolymers[7] which were abbreviated as 20K*XX*, where 20K refers to the M_n of the PEO block and *XX* refers to the degree of polymerization of the PBLA block estimated by ^{1}H NMR to be 18, 25, 32, and 55. 20K18, 20K25, and 20K32 had nearly monodispersed chain lengths (molecular weight polydispersity: M_w/M_n = 1.04, 1.04, and 1.07, respectively), while 20K55 showed a polydispersity of 1.36 wider than others used here but narrow to use as a fine material.[7]

All copolymers were soluble in dichloromethane, DMSO, and DMF but were insoluble in water. If the DMSO solution of the copolymers (1 g L^{-1}, 1 mL) was poured into pure water (5 mL), colloidal solutions containing particles with a diameter of 50−150 nm (measured by dynamic light scattering particle size analyzer, LB-500 HORIBA) were created, suggesting that the copolymers had a self-assembling nature in water. However, it was impossible to obtain a continuous hydrogel membrane by casting the colloidal solution. Therefore, we performed in situ hydrogelation; films (thickness: 0.01 mm) cast from methylene chloride solutions of the copolymers were immersed into pure water to yield almost transparent hydrogel membranes with thickness of 0.01−0.02 mm. The films swelled smoothly and rapidly, and the swelling equilibrated within 10 min. The degree of swelling, q, was 5.8 for 20K18, 5.4 for 20K25, 4.4 for 20K32, and 2.4 for 20K55, decreasing with an increasing hydrophobic PBLA content, which corresponds to the water content ranging 58−83 wt %. In Figure 1, one can see the external appearance of the 20K25 hydrogel membrane. If the hydrogels swelled sufficiently in water, they automatically rolled up, presumably due to their high flexibility and the minimization of the surface energy (Figure 1a). The hydrogel membrane could be easily picked up into the atmosphere without breaking and in addition could be expanded by a pair of tweezers. As a result, the hydrogel thin membrane could rest stably on two rods with an interval of 1 cm (Figure 1b). All of the hydrogels membranes prepared here were tough and underwent large deformations without breaking in their equilibrated water-swollen state. On the other hand, the PBLA and PEO homopolymers and their mixtures did not give rise to a continuous hydrogel membrane. In addition, poly{EO-*block*-BLA} and other diblock amphipathic macromolecules formed micelles in water but never formed a continuous membrane.[10,11] This comparison shows the significance of the hydrophobic−hydrophilic−hydrophobic triblock architecture, presumably since the interchain interactions can occur over a number of macromolecular chains to create the continuous hydrogel membranes.

2. Hydrogel Structures. We investigated the hydrogel structures by microscopy, spectroscopy, X-ray diffraction, and TEM to elucidate the mechanism of the hydrogel toughening. Figure 2 shows crossed-polarizing photomicrographs of the hydrogels. In thin hydrogel membranes of all compositions, we observed giant crystalline domains with a spherullite morphology, sized from 10 μm to 4 mm, increasing with a decrease in the PBLA content. Although the upper limit of the one-shot microscopic view makes it impossible to show spherullites scaled more than 1 mm in this figure, we directly observed spherullites with diameters of 1−4 mm in the 20K18 and 20K25 hydrogels by sliding a microscope stage. In particular, the 20K18, 20K25, and 20K32 hydrogels formed spherullites showing clear Maltese crosses and boundaries as widely seen in the single spherullites of low-molecular-weight molecules.[12] The vague spherullite boundary in the 20K55 sample seen in Figure 2d may be associated with its wider molecular weight distribution and longer molecular length as compared to the other copolymers. This spherullite pattern indicates a continuous radial variation of the orientation of the copolymer crystal axes. Thus, the crystals of the triblock chains in the hydrogels were arranged in a millimeter-scaled continuous length. According to reports on partially crystallized hydrogels such as regenerated cellulose[5] and polyacrylates with long alkyl side chains,[4] only the nanosized crystalline domains were formed. The formation of giant crystalline domains whose size reached the millimeter scale in the water-swollen state is quite unique and surprising. The present spherullites were easily deformed by external mechanical force, implying that the spherullites contained water. The spherullites were generally composed of polycrystallites arranging radially, and in the clear areas of the crystallites, amorphous domains are

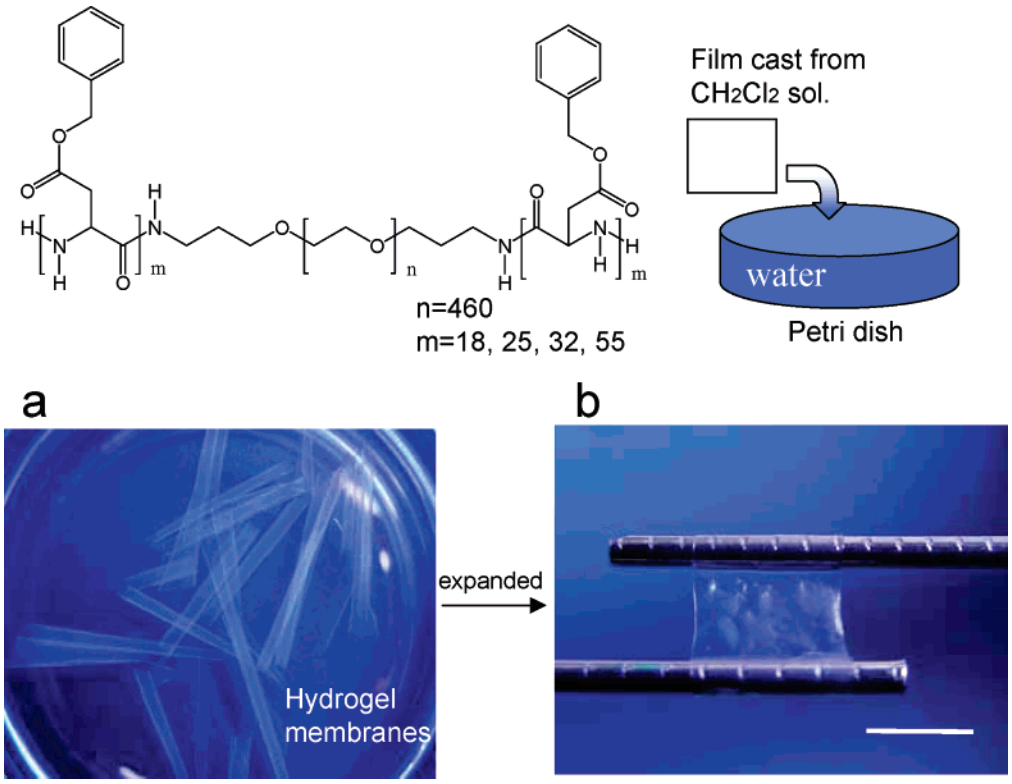

Figure 1. Molecular structure of the poly{(γ-benzyl L-aspartate) (BLA)-*block*-ethylene oxide (EO)-*block*-BLA}s and its hydrogelation procedure (top) and the external appearance of the representative hydrogel of 20K25. (a) In water. (b) In the atomosphere. Scale bar: 1 cm.

present.[12] This specific arrangement makes it possible to form the millimeter scaled continuous domains of the spherullites. In the case of the present hydrogels, the hydrophobic−hydrophilic−hydrophobic triblock hydrogels may adopt a specific radial arrangement of the crystalline domains with the hydrated PEO domain.

Figure 3a shows wide-angle X-ray diffraction (WAXD) diagrams of the hydrogels in their water-swollen state. One can see that a distinct peak appeared at $2\theta = 21°$ for 20K18, $2\theta = 21°$ for 20K25, $2\theta = 23°$ for 20K32, and $2\theta = 23°$ for 20K55 (θ: diffraction angle), corresponding to short-range spacings (d_1) of 0.42, 0.42, 0.39, and 0.39 nm, respectively, indicating that every membrane formed a crystalline structure at the molecular level. The diffraction at $2\theta = 21°$ in the 20K18 and 20K25 hydrogels was not observed in the WAXD pattern of the copolymer dry film {$2\theta = 5.9°$ (1.5 nm), 19° (0.47 nm), and 23° (0.39 nm)},[6] suggesting that water intrusion induced a crystal−crystal transformation of the triblock chains. Since the PBLA block is hydrophobic, the distinct peaks in the WAXD diagram may be associated with the crystals of PBLA. However, the α-helical PBLA chain usually showed a peak at $2\theta = 5.9°$[6] where no peak appeared. Thus, the diffraction at $2\theta = 21°$ may be due to another PBLA conformation, since the PBLA chain has a wide variety of conformations.[13,14] On the other hand, the diffraction at $2\theta = 23°$ in the 20K32 and 20K55 hydrogels lies at the same angle as the largest diffraction peak of the PEO crystals,[6] suggesting that the PEO crystals remained in a water-swollen state. We performed a simple water intrusion test into the hydrogel structure; the dry film was immersed into an aqueous solution of the pigment Congo red (10^{-4} M) on the microscope stage, and we observed that the red solution intruded smoothly into the spherullite domains. This observation indicates that the PEO segments in 20K32 and 20K55 are capable of hydrating. The WAXD peak may be due to the PEO crystals buried in the hydrophobic domains of PBLA with longer chains. Additionally, we observed the temperature dependence of crossed-polarizing texture for spherullites at a heating rate of 10 °C min^{-1} (Mettler Toledo FP82HT hot stage). The sample brightness under the crossed-polarizer showed a slight reduction at 60 °C in the 20K55 and 20K32 hydrogel membranes while no change in 20K18 and 20K25 although DSC thermograms showed no peak in the temperature range of 20−95 °C. The brightness change may be due to the melting of the PEG domains which are too small to show a distinct endotherm in water. On the other hand, the spherullites shape and boundary keep clear in the temperature range of 20−95 °C. This stability may be associated with the intrinsic properties of PBLA which shows a high denaturation temperature of around 150 °C. Here, we observed that the 20K55 hydrogel also showed a very small WAXD diffraction at $2\theta = 21°$. According to the literature, the crystals of the peptides and oriented silklike fibers adopting the β-sheet structure showed some diffractions containing the strongest peak at $2\theta = 21°$, suggesting that the present hydrogel membranes may adopt the β-sheet structure.[15,16]

Figure 3b shows small-angle X-ray diffraction (SAXD) diagrams of the hydrogel thin membranes in their water-swollen state. The water-swollen membranes produced a large and broad peak at around $2\theta = 0.19°$ for 20K18, $2\theta = 0.16°$ for 20K25, $2\theta = 0.17°$ for 20K32, and $2\theta = 0.13°$ for 20K55, corresponding to long-range spacings (d_2) of about 46, 55, 52, and 68 nm, respectively. The SAXD peaks could be detected here for the first time, owing to the reduced thickness, while the thick membrane (more than 0.1 mm thickness) reported previously showed no distinct peak presumably due to

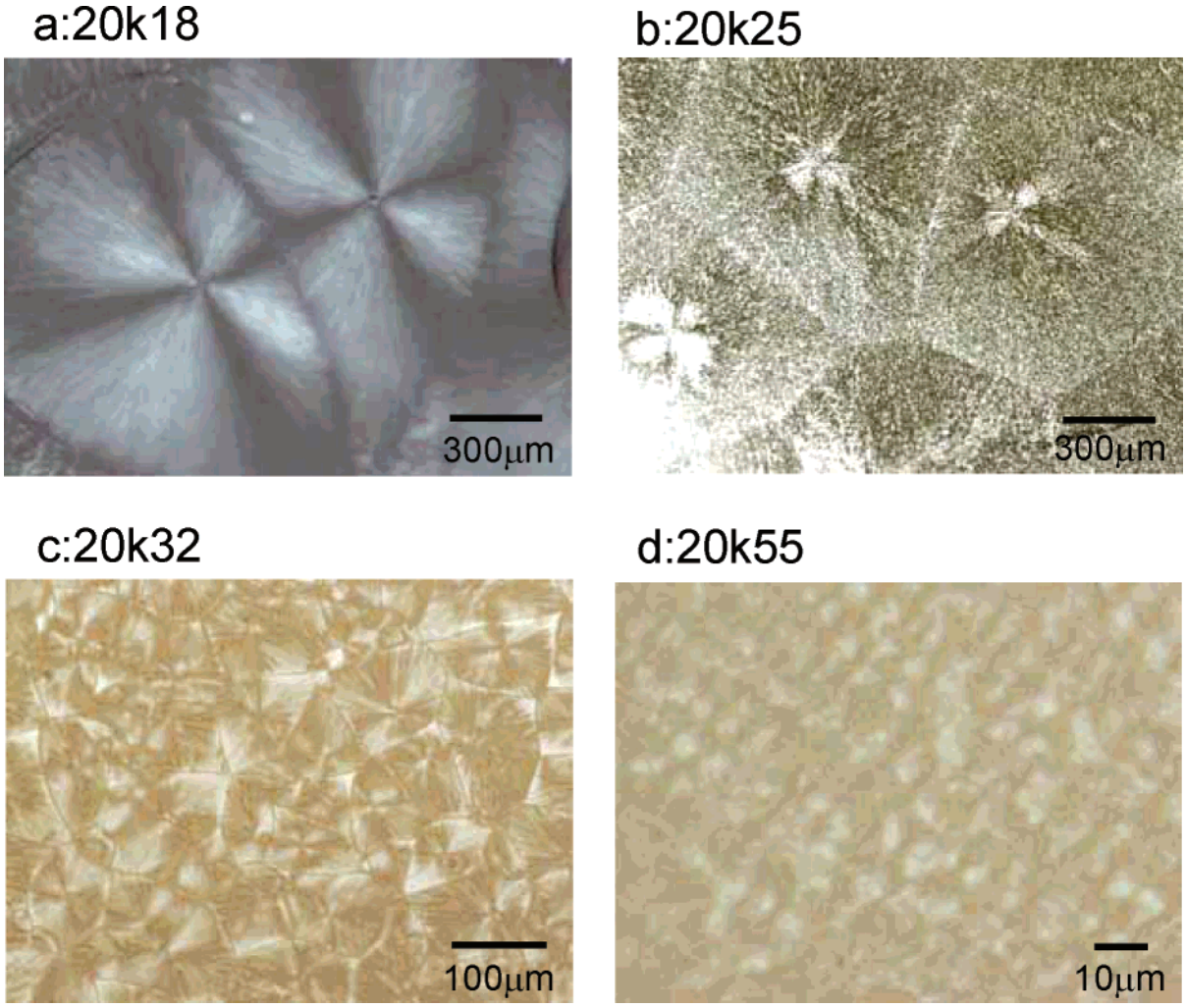

Figure 2. Crossed-polarizing microscopic images of the hydrogel thin membranes in the equilibrated water-swollen state.

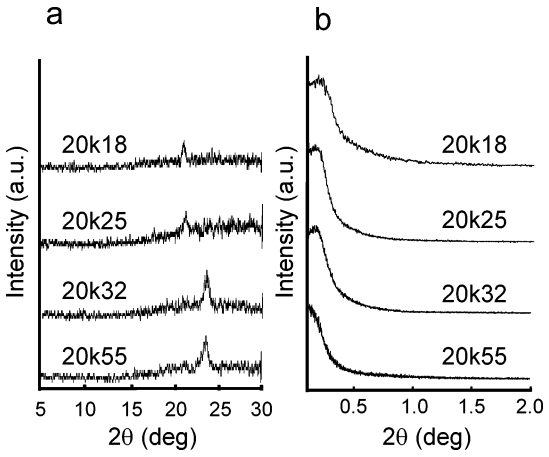

Figure 3. X-ray diffraction diagrams of the hydrogel membranes in the equilibrated water-swollen states: (a) wide-angle X-ray diffraction diagrams; (b) small-angle X-ray diffraction diagrams.

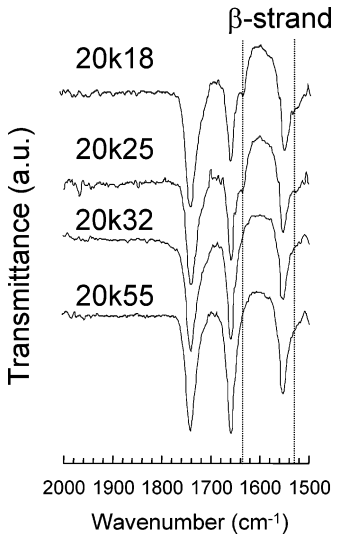

Figure 4. Fourier transformed infrared spectra, FT-IR, of the hydrogels in the equilibrated water-swollen states. Water molecule IR peaks were subtracted. The dotted lines refer to β-strand peaks.

redundant multiscattering inside the membrane. On the other hand, the SAXD peaks of the dried films did not appear or were very weak, as described in a previous paper.[6] These results indicate that the water induced the formation of long-range structures.

Figure 4 shows Fourier transformed infrared (FT-IR) spectra of the hydrogels in their equilibrated water-swollen state. As described in the former section, the dry copolymers had vibrations at the following wavenumbers: 1736 cm^{-1} (s, C=O), 1657 cm^{-1} (s, amide I), and 1552 cm^{-1} (s, amide II), indicating that the PBLA segments adopted a right-handed α-helical conformation according to the literature.[13] On the other hand, the other small vibration peak at 1635 cm^{-1} (amide I) and the shoulder at 1531 cm^{-1} (amide II) assigned to β-sheet

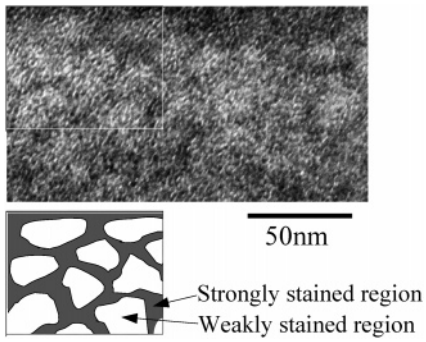

Figure 5. Transmission electron microscopic (TEM) image of stained ultrathin cross sections for 20K25 dry sample. The freeze-dried film embedded in the epoxide resin was cut in a microtome system to yield the ultrathin cross sections with a thickness less than 0.1 μm, followed by RuO_4 staining. The stainning contrast was explained using the schematic illustration shown at the bottom.

strands[13] also appeared in the water-swollen samples (Figure 4), indicating the water-induced transformation of an α-helix to a β-sheet within a small region of the PBLA chains. In the dry state, the α−β transformation also occurred within the PEO block melting upon heating.[6] Moreover, a similar thermal α−β transformation has been reported in the case of Alzheimer's β-amyloid protein.[17] This α−β transformation can occur when the polypeptide chains gain high mobility. In the present case, the PBLA chain can gain mobility at the interface with the water-swollen domain. We can assume that the PBLA β-strand can exist around the connecting region with the hydrated PEO block. The β-strand composition to the whole PBLA chain was estimated from the peak area ratio of 1657 cm^{-1} to 1635 cm^{-1} using peak fitting software (GRAMS/AI ver.7, Thermo Galactic) to be 21% for 20K18 (7.6 units), 31% for 20K25 (15.5 units), 5.6% for 20K32 (3.6 units), and 9.8% for 20K55 (10.8 units). The β-sheet composition was low in every copolymer, supporting the assumption described above. It is noted that the β-sheet composition of the 20K32 and 20K55 hydrogels was relatively low as compared to 20K18 and 20K25. This difference may be associated with the difference in the short-range structure proposed by the WAXD study. The new WAXD diffraction ($2\theta = 21°$) of the 20K18 and 20K25 hydrogels may be assigned to the β-sheet arrangement, which has a structural periodicity of about 0.47 nm.[15,16] This diffraction was not detected in the 20K32 hydrogel, presumably due to the low composition of β-structures, but was faintly detectable in the 20K55 hydrogel with a β-sheet-composing units more than 20K32. According to the literature,[13] PBLA cooperatively forms interchain hydrogen bonds in the β-state, which may be effective in enhancing the hydrogel toughness.

To investigate the morphology of the long-range structure, we made a TEM observation of ultrathin cross sections with less than 0.1 μm thickness for 20K25 (Figure 5). The specimen was stained by RuO_4. One can see the staining contrast of sea−island structure; strongly stained region forms a continuous network phase (sea) with a thickness of 8−10 nm and weakly stained regions (island) with a size of 20−30 nm lie scattered, as schematically shown by the illustration below the TEM image. Since RuO_4 positively stain both blocks of PBLA and PEO, the staining contrast may be due to the density difference between these blocks. Since the molecular weight of PEO block is much higher than that

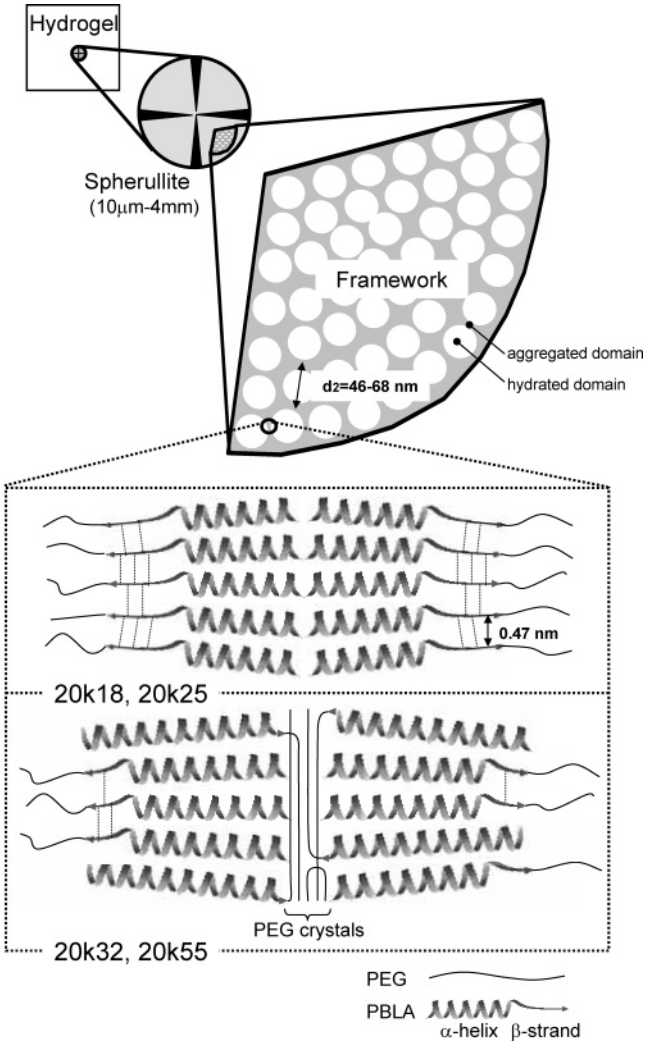

Figure 6. Schematic illustration of the hydrogel structure proposed on the basis of the data of microscope, FT-IR, and X-ray diffraction studies. The hydrogel membrane has many spherullites with a framework consisted of the water domains (hydrated PEO) and the aggregated domains which are comprised of PBLA crystallites with α- and β-conformation in 20K18 and 20K25 and comprised of both PBLA and PEO crystallites in 20K32 and 20K55.

of PBLA blocks and the size of island region is larger than the thickness of the sea regions, we can presume that sea and island correspond to PBLA and PEO blocks, respectively. In the water-swollen state, the hydrophilic PEO region can swell while the hydrophobic PBLA region can keep the continuous network structure. The results of the X-ray diffraction, FT-IR, and TEM studies indicated that the hydrogels showed a crystal−crystal transformation (WAXD) accompanied by an α-helix−β-sheet PBLA transformation (FT-IR) and also formed a long-range structure with d_2 spacing confirmed by the SAXD study during the water swelling. Since the long-range structure was formed by water intrusion, one can assume that it should be related to a segregation of the water-swollen region (PEO island) and the hydrophobically aggregated region (PBLA sea). The SAXD diagram showed no satellite diffraction, indicating that the long-range diffraction was attributed to only a nonspecific hexatic arrangement. We propose a framework structure formation in the spherullites of the hydrogel membrane, as shown in Figure 6. In this framework, the water-swollen domains of the PEO

islands lie scattered and must be surrounded by the hydrophobic sea domains of the PBLA blocks. Because of the hydrophobic−hydrophilic−hydrophobic architecture, every island should be continuously cross-linked over the spherullite domain by the PBLA hydrophobic sea networks. The PEO block (PD = 460) is 115 nm long when in its fully extended conformation (0.25 nm per a unit), which seems to be long enough to form water-swollen islands arranged at intervals of $d_2 = 46-68$ nm. The PBLA block length of 20K25 is estimated as $d_{PBLA} = 9.5$ nm in both sides (50 units), using the data of a 0.54 nm α-helix length per 1 cycle (3.6 unit), a 0.25 nm β-strand length per 1 unit, and 31% β-compositions. d_{PBLA} is in a good agreement with the sea thickness of TEM image, suggesting that the PBLA domains formed a bilayer structure as shown in Figure 6. Subtraction of the PBLA block lengths from the d_2 spacings (55 nm) gave diameters of the water domain as 45.5 nm. If the water domains are spherical, then their volumes (V_{water}) can be calculated as 4.9×10^4 nm^3, which can shrink down to 9.1×10^3 nm^3 by drying. On the other hand, the islands of TEM image had volumes ranging from 4.2×10^3 to1.4×10^4 nm^3 by a rough calculation under hemispherical approximation. This volume range corresponds to 9.1×10^3 nm^3 the calculated value from d_2 and PBLA length, which strongly suggest that the framework structure shown in Figure 6 is quite reliable. If the water domain was cylindrical morphology, the volume became much higher than that calculated from the TEM image. As a result, the water domain may be spherical and surrounded by the continuous hydrophobic network domain of PBLA bilayer within the giant spherullites. Although we performed the TEM observation of other samples repeatedly, we failed to find the suitable staining condition. We presumed that other samples formed the analogous structure because of the distinct SAXS peak similar to 20K25.

The multiple hydrogen bonds of the β-sheet structure of PBLA with a periodicity of 0.47 nm may support the frameworks. Since WAXD of 20K18 showed the peak at the same diffraction angle as that of 20K25, 20K18 may form the bilayer structure similar to 20K25. On the other hand, since WAXD peaks of 20K32 and 20K55 hydrogels demonstrated that PEO crystallites remained in the water-swollen state, they did not form such a simple bilayer structure. Since hydrophilic PEO blocks cannot form the crystallites when exposed to the water, PEO crystallites may be present in the PBLA aggregated domain. In this case, some PBLA chains of 20K32 and 20K55 should lie inversely differently from the 20K18 and 20K25 models, as shown in the bottom illustration of Figure 6. This inverse arrangement of PBLA reduces the amount of PEO in the water domain to a lowered q, which is consistent with the observed phenomenon. Furthermore, PBLA cannot show a α−β transformation because the chain mobility does not increase, which is consistent with the FT-IR results. These findings also support the validity of the framework structure.

3. Mechanical Properties. As shown in Figure 7, all of the hydrogels had a stress−strain curve with a positive convex shape, unlike conventional soft hydrogels but more like conventional plastic films. The Young's modulus (E) of the 20K25, 20K32, and 20K55 hydrogels ranged between 1.5, 2.5, and 9.1 MPa, respectively, increasing with an increase in the polymerization degree of the PBLA segments. As a result,

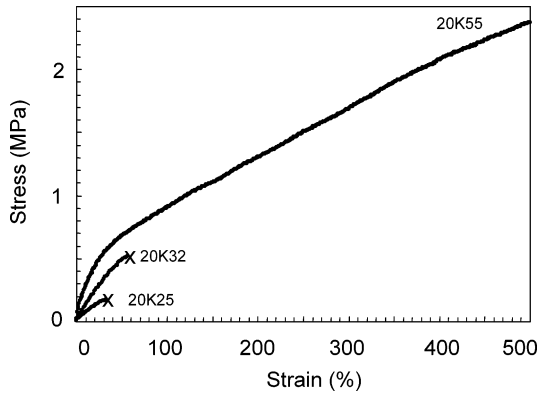

Figure 7. Stress−strain curves of the hydrogel membranes in the equilibrated water-swollen state. The crosses show the point of mechanical failure.

20K25, 20K32, and 20K55 yielded self-sustaining, thin hydrogel membranes (thickness: 0.01−0.02 mm). The 20K18 hydrogel film was too fragile to measure any tensile data, although it was also self-sustaining. The high E values in 20K55 may be due to the enhanced hydrophobic aggregation of the longer PBLA segments than other samples, since the dry copolymers with the higher molecular weight showed the higher E.[6] In the hydrogel membranes, the deformation resistance of the hydrophobic continuous domain may dominate the value of E since the hydrated PEO domains may be very soft. Since the 20K55 hydrogel can have the thick hydrophobic domain predicted by the long d_2 value and long PBLA segment, it showed a high E value. Additionally, only 20K55 formed PEO crystals and long β-sheet structures which are both mechanically supporting structures. In particular, the E of the 20K55 membrane exceeded twice the value of dialysis membranes composed of regenerated cellulose (Spectra/Por 7 membrane, Spectrum Laboratories Inc., thickness; 60 μm, $q = 3.7$, $E = 4.1$ MPa). Curiously, the hydrogel's molecular weight was not high, the membrane was very thin, and the PEO segment was very flexible, whereas the regenerated celluloses have rigid saccharine rings in an extremely long chain. The maximal strength of the hydrogel films was 0.17, 0.52, and >5.5 MPa for 20K25, 20K32, and 20K55, respectively, and were high relative to conventional physical hydrogels (0.02−0.3 MPa).[3] The specific maximal strength increased with an increase in PBLA composition, indicating that the intrinsic strength of the polymer chains was enhanced by the PBLA segments' hydrophobicity as organized by the surrounding water. Mechanical failure of 20K25 and 20K32 was observed at low strains of 35% and 55%, respectively, whereas 20K55 was not broken at a strain of 500%, which is the upper limit of the apparatus. The breaking occurred at the boundary of the spherullites confirmed by the microscopic observation of the broken samples. 20K55 hydrogels have a vague boundary line beyond which we can guess that some triblock chains can intercalate to make the structural continuous length longer, different from the other hydrogels, which may be one possible reason for the higher elongation.

4. Conclusions. ABA-type triblock copolymers, poly{(γ-benzyl L-aspartate) (BLA)-*block*-ethylene oxide (EO)-*block*-BLA}, with controlled chain lengths were precisely prepared. The copolymers have a hydrophobic−hydrophilic−hydrophobic architecture with long hydrophilic blocks (PD of PEO = 460). The copolymer film (ca. 0.01 mm thickness) was immersed into water to yield self-

sustaining, thin hydrogel membranes (0.01−0.02 mm thickness), which were largely deformable and tough in their equilibrated water-swollen state. Crossed-polarizing microscopy confirmed that the water-swollen membrane had a framework of giant crystalline domains sized in 10 μm−4 mm. During the water-swelling process, the triblock copolymers showed a α-helix−β-strand transformation of the PBLA blocks and long-range structure formation. On the basis of the results of the microscopic, FT-IR, and X-ray diffraction studies, a framework structure where the aggregated domains lie in a continuous network and surround the water domain can be proposed. This structural models showed an excellent agreement between calculated and observed values of swelling degrees. This framework reinforces the thin hydrogel membrane, thus increasing the toughness. Every hydrogel membrane was self-sustaining in the atmosphere. As a result of mechanical testing, the 20K55 hydrogels showed excellent properties exceeding Young's modulus of a regenerated cellulose membrane, high strength, and high elongation. Thus, the excellent mechanical strength of physically cross-linked, thin hydrogel membranes with good cell compatibility[7] may yield a new type of wet biomaterial sheet with added ease of handling. Furthermore, other functions such as selective molecular transportation using PBLA helical chirality and specific photomanipulation by changing the spherullitic molecular orientation can be expected in future work.

Acknowledgment. This study was financially supported in part by NOF Corp., Japan, and The Association for the Progress of the New Chemistry. We also show an appreciation to Mr. Taiki Shimokuri (Osaka University, Japan) for valuable discussion.

References and Notes

(1) (a) Dusek, K., Ed.; *Advances in Polymer Science*; Springer-Verlag: Berlin, 1993; Vol. 109. (b) Dusek, K., Ed.; *Advances in Polymer Science*; Springer-Verlag: Berlin, 1993; Vol. 110.

(2) (a) Clark, A. H.; Ross-Murphy, S. B. *Adv. Polym. Sci.* **1987**, *83*, 57. (b) Miyazaki, T.; Yamaoka, K.; Kaneko, T.; Gong, J. P.; Osada, Y. *Sci. Technol. Adv. Mater.* **2000**, *1*, 201.

(3) Gong, J. P.; Katsuyama, Y.; Kurokawa, T.; Osada, Y. *Adv. Mater.* **2003**, *15*, 1155.

(4) (a) Osada, Y.; Matsuda, A. *Nature (London)* **1995**, *376*, 219. (b) Kaneko, T.; Yamaoka, K.; Gong, J. P.; Osada, Y. *Macromolecules* **2004**, 37, 5385.

(5) Williams, A., Phillips, G. O., O'Phillips, G., Eds.; *Cellulose and Cellulose Derivatives: Physico-Chemical Aspects and Industrial Applications*; Technomic Publishing Co.: Lancaster, 1995.

(6) Tanaka, S.; Ogura, A.; Kaneko, T.; Murata, Y.; Akashi, M. *Macromolecules* **2004**, *37*, 1370.

(7) Tanaka, S.; Ogura, A.; Kaneko, T.; Murata, Y.; Akashi, M. *Biomacromolecules* **2004**, *5*, 2447.

(8) (a) Perret, R.; Skoulios, A. *Makromol Chem.* **1972**, *156*, 143. (b) Bogdanov, B.; Vidts, A.; Schacht, E.; Berghmans, H. *Macromolecules* **1999**, *32*, 726. (c) Kugo, K.; Uno, T.; Yamano, H.; Nishino, J.; Hideo, M. *Kobunshi Ronbunshu* **1985**, *42*, 731. (d) Floudas, G.; Papadopoulos, P.; Klok, H.-A.; Vandermeulen, G. W. M.; Rodrigues-Hernandez, J. *Macromolecules* **2003**, *36*, 3673. (e) Arnal, M. L.; Lopez-Carrasquero, F.; Laredo, E.; Muller, A. J. *Eur. Polym. J.* **2004**, *40*, 1461.

(9) Fuller, W. D.; Verlander, M. S.; Goodman, M. *Biopolymers* **1976**, *15*, 869.

(10) Harada, A.; Kataoka, K. *Science* **1999**, *283*, 65.

(11) Kataoka, K.; Harada, A.; Nagasaki, Y. *Adv. Drug Delivery Rev.* **2001**, *47*, 113.

(12) Schultz, J. M. *Polymer Crystallization: The Development of Crystalline Order in Thermoplastic Polymers*; American Chemical Society: Washington, DC, 2001.

(13) Das, K. J. M.; Rastogi, S.; Tandon, P.; Gupta, V. D. *Eur. Polym. J.* **2001**, *37*, 2295.

(14) Karlson, R. H.; Norland, K. S.; Fasman, G. D.; Blout, E. R. *J. Am. Chem. Soc.* **1960**, *82*, 2268.

(15) Winningham, M. J.; Sogah, D. Y. *Macromolecules* **1997**, *30*, 862−876.

(16) Wainwright, S. A.; Biggs, W. D.; Currey, J. D.; Gosline, J. M. *Mechanical Design in Organisms*; Princeton University Press: Princeton, NJ, 1976; Chapters 3 and 4.

(17) Chu, H. L.; Lin, S. Y. *Biophys. Chem.* **2001**, *89*, 173.

MA050121P